This is a repository copy of *Alveolar macrophage apoptosis-associated bacterial killing helps prevent murine pneumonia*.

White Rose Research Online URL for this paper:
https://eprints.whiterose.ac.uk/141496/

Version: Supplemental Material

Article:

Preston, J.A., Bewley, M.A., Marriott, H.M. orcid.org/0000-0003-1070-0054 et al. (15 more authors) (2019) Alveolar macrophage apoptosis-associated bacterial killing helps prevent murine pneumonia. American Journal of Respiratory and Critical Care Medicine, 200 (1). pp. 84-97. ISSN 1073-449X

https://doi.org/10.1164/rccm.201804-0646OC

© 2019 American Thoracic Society. This is an author produced version of a paper subsequently published in American Journal of Respiratory and Critical Care Medicine. Uploaded in accordance with the publisher's self-archiving policy.

Reuse
Items deposited in White Rose Research Online are protected by copyright, with all rights reserved unless indicated otherwise. They may be downloaded and/or printed for private study, or other acts as permitted by national copyright laws. The publisher or other rights holders may allow further reproduction and re-use of the full text version. This is indicated by the licence information on the White Rose Research Online record for the item.

Takedown
If you consider content in White Rose Research Online to be in breach of UK law, please notify us by emailing eprints@whiterose.ac.uk including the URL of the record and the reason for the withdrawal request.

eprints@whiterose.ac.uk
https://eprints.whiterose.ac.uk/

1 **Alveolar macrophage apoptosis-associated bacterial killing helps prevent murine**
2 **pneumonia.**
3

4 Julie A. Preston, Martin A. Bewley, Helen M. Marriott, A. McGarry Houghton,
5 Mohammed Mohasin, Jamil Jubrail, Lucy Morris, Yvonne L. Stephenson, Simon
6 Cross, David R. Greaves, Ruth W. Craig, Nicovan Rooijen, Colin D. Bingle, Robert
7 C. Read , Timothy J. Mitchell, Moira K.B. Whyte, Steven D. Shapiro and David H.
8 Dockrell
9
10

11 # On Line Supplement

Supplemental Methods.

Bacteria

Serotype 2 S. *pneumoniae* (D39 strain, NCTC 7466) was grown as previously described(1). Serotype 1 *S. pneumoniae* (WHO reference laboratory strain SSISP 1/1: Statens Seruminstitut) was also grown as previously described and was used for *in vivo* infection(2). A streptomycin resistant derivative of D39 (FP58) (3) was obtained from Prof. Timothy Mitchell University of Birmingham. For experiments on human cells, *S. pneumoniae* strains were opsonized in RPMI (Sigma-Aldrich) containing 10% human anti-pneumococcal immune serum as previously described (1) or for murine cells with murine serum containing detectable anti-pneumococcal antibodies (4). *Haemophilus influenzae* type b Eagan strain (H636) was obtained from Dr Derek Hood, University of Oxford. *Staphylococcus aureus* Newman strain and a kanamycin resistant Newman strain were obtained from Prof. Simon Foster, University of Sheffield. All infections were carried out at a multiplicity of infection (MOI) of 10, to ensure a level of intracellular bacteria that triggered apoptosis and overwhelmed initial phagolysosomal killing mechanisms, except with *S. aureus* where lower MOI were used due to higher levels of initial ingestion. After challenge, extracellular bacteria where washed off after 4 h, and media replaced.

Isolation and culture of macrophages and other leukocytes

Bone marrow-derived macrophages (BMDM) were obtained by culturing marrow for 14 days as previously described (2). Differentiation was confirmed by expression of F4/80. Resident alveolar macrophages (AM) were collected by bronchoalveolar lavage (BAL) with 4 aliquots of 0.8ml PBS. Peritoneal macrophages (PM) were collected 4 days after i.p. injection of 4% thioglycollate (5). AM and PM were enriched by 4 h

plastic adherence in RPMI (Lonza) + 10% FCS with low LPS. Murine neutrophils were isolated from peripheral blood using negative immunomagnetic selection as previously described (6), while murine $CD19^+$ B-lymphocytes and $CD3^+$ T-lymphocytes were isolated using a fluorescent cell sorter (FACSAria, BD Biosciences). Human monocyte-derived macrophages (MDM) were isolated from whole blood donated by healthy volunteers as previously described (1). In some experiments apoptosis was induced *in vitro* by UV irradiation (120mJ/cm^2, Stratalinker 1800, Stratagene). As indicated macrophages were incubated with 50 μM 1400W (Calbiochem), an inhibitor of iNOS, 50 μM Trolox (Calbiochem), an antioxidant, or 1 mM Mito-TEMPO (Enzo), an inhibitor of mitochondrial ROS or 50 μM zVADfmk (Enzymes Systems Products), an inhibitor of caspases or 50 μM zFAfmk (Enzyme Systems Products) as zVADfmk's control from 1 h prior to bacterial challenge and for the duration of bacterial exposure.

In vivo infection

Mcl-1 transgenic mice and non-transgenic littermates, from the same cages, were inoculated with bacteria and tissues collected to determine viable bacteria, neutrophils in lavage cytospins and apoptotic macrophages in lavage cytospins or by analysis of flow cytometry as previously described (2).

Bone marrow transfer

Recipient mice were 6 week old C57BL/6J female mice (Charles River), maintained on acidified water in individual ventilated cages and irradiated with 2 doses of 550 rads separated by 4 h. Donor bone marrow, was obtained from CD68.hMcl-1^+ transgenic mice, or CD68.hMcl-1^- non-transgenic littermates, that had been backcrossed for 10 generations onto a C57BL/6J background. Bone marrow was isolated as described

previously (7) and resuspended in HBSS at approximately 1×10^7 cells/ml. 4 h after the second dose of radiation, 200 µl of the bone marrow cell suspension was injected into each recipient mouse via the tail vein. The mice were maintained in individual ventilated cages with free access to autoclaved food and acidified water for 3 months before intratracheal instillation with 1×10^4 colony forming units of type 1 *S. pneumoniae* as described. We have previously documented that at this time point post-transplantation this protocol allows replacement of recipient alveolar macrophages with donor macrophages (8). We and others have also shown that the function of alveolar macrophages is reduced by the transplantation procedure and mice are more susceptible to infection with a given dose after transplantation and less able to effectively clear all bacteria when challenged with an inoculum mice that have not undergone an adoptive transplant procedure would have cleared (8, 9). Following adoptive bone marrow transfer, macrophage-associated bacteria were assessed by cytospin.

Neutrophil Depletion

Mcl-1 transgenic mice and non-transgenic littermates were injected i.p. with 200µg Ly6G specific antibody (eBioscience, functional grade, clone 1A8) to deplete circulating neutrophils 24h before intratracheal inoculation with 10^4 colony forming units of type 1 pneumococci.

Flow Cytometry

To detect murine cell surface markers, cells were incubated with 1µg ml^{-1} F4/80-FITC (rat monoclonal IgG2b, clone CI:A3-1, AbD Serotec), CD19-PE (rat monoclonal, IgG2aK clone 1D3, BD Pharmingen), CD3-PE (rat monoclonal, IgG2bK clone 17A2, BD Pharmingen). In other experiments, cells were incubated with either 10 µM 5,5′,6,6′-tetrachloro-1,1′,3,3′- tetraethylbenzimidazolylcarbocyanine iodide (JC-1;

Molecular Probes) to measure loss of inner mitochondrial transmembrane potential ($\Delta\psi_m$) (8), RPMI containing 5 μM acridine orange (Sigma-Aldrich) to measure loss of lysosomal acidification (LLA) (8). Cells were incubated in phenol-red free RPMI containing 5 μM difluorescein diacetate (DAF-FM) (Sigma) to measure NO (10). Caspase activity in live cells was analyzed using the CellEvent caspase 3/7 green flow kit (Life Technologies). ROS were measured using 2′, 7′-dichloro-dihydrofluorescein diacetate (DCFDA; Sigma-Aldrich) (11) and mROS with MitoSOX-red (Invitrogen) (12). Flow cytometric measurements were performed using a four colour FACSCalibur (Becton Dickinson). Cell sorting was performed on a FACSAria (Becton Dickinson). Samples were resuspended in 200 μL PBS, and forward and side scatter light was used to identify cell populations and at least 10,000 events recorded All data was analysed using FlowJo software, version 8.8.4 (Tree Star Inc.).

Confocal microscopy.

Streptococcus pneumoniae (D39) were labelled with Alexa Fluor-647 tagged carboxylic acid succinimidyl ester as described previously (12, 13). Briefly, frozen aliquots of bacteria were thawed out and resuspended in PBS at a cell density of 100 million colonies forming units per mL. A 500 μL aliquot was removed, and 18.8μL of 0.5 mg/mL Alexa Fluor-647 carboxylic acid succinimidyl ester (Life Technologies) in DMSO (Sigma Aldrich) was added and incubated in the dark for 1 h at room temperature. The suspension was then centrifuged at 2000*g* for 10 min, the supernatant was discarded, and the cell pellet was resuspended in 500 μL of PBS and opsonized with 10% mouse immunized pool serum for 30 min at 37°C. Macrophages were challenged with labelled or vehicle treated bacteria as described (2), and at 16 h post-challenge were stained with 10 μM DAF-FM diacetate (Molecular probes, D23842) in

1 serum and phenol red free RPMI media for 30 min at 37°C and then 2.5 μM MitoSOX-
2 red (Invitrogen) to detect mROS for 25 min at 37°C. To perform co-staining with
3 phagolysomes and ER after 16 h of bacterial challenge, macrophages were stained with
4 or without DAF-FM, followed by MitoSOX-red , and then 1.0 μM cresyl violet acetate
5 (Sigma, C10510540) for 20 min to detect lysosomes/phagolysosomes (2, 14) or 1.0 mM
6 ER tracker red (Bodipy TR Glibenclamide, Life Technologies, E34250) for 20 min at
7 37°C. Cells were then washed in HBSS three times, before being fixed in 2%
8 paraformaldehyde. Cells were visualised using a 488 nm excitation and 500-530 nm
9 emission detector for DAF-FM diacetate, 543 nm excitation and 565-615 nm emission
10 detector for MitoSOX-red, 633 nm excitation, 640-704.2 nm emission for Alexa Fluor-
11 647 carboxylic acid succinimidyl ester and cresyl violet, 543 nm excitation and 560 nm
12 emission detector for ER tracker red with a Axiovert 200M Zeiss LSM510 inverted
13 confocal fluorescence microscope using a 63x1.4 NA oil objective lens. Representative
14 confocal images (supplementary Figures E4-6) were created from the region of interests
15 (ROI) of maximum projected z-sections images (Size scaling: 0.07x0.07x0.48μm,
16 Scan zoom 2 and average line 4) using a 17x17 hat filter with intermodal black and
17 white threshold correction by ImageJ, as described previously (15). The Pearson's
18 correlation coefficient was calculated as described previously in (16). The corrected
19 integrated total cell fluorescence intensity for NO and mROS were quantified using
20 ImageJ (v1.48, NIH), as described previously by McCloy RA *et al.*, (17). Briefly, the
21 individual channels for Z-sections images were separated and the maximum Z-
22 projected images were generated by ImageJ (*e.g.* Image>Stack>Z projected).
23 Subsequently, the corrected integrated total cell fluorescence was calculated using the
24 following formula, the corrected total cell fluorescence (CTCF) = integrated density –
25 (area of selected cell × mean fluorescence of background readings), as calculated from

1 the free-hand selected outline for each cell. Similarly, a ROI was selected from the
2 separated channel-1 or channel-2 images to quantify the correlation coefficient for NO
3 versus mROS or phagolysosome fluorescence and NO versus mROS or bacteria as
4 described (15). The digital distance between NO and mROS or bacteria or
5 phagolysosomes or between ER and NO or bacteria or phagolysosomes was measured
6 by ImageJ. From this analysis, the signals were classified as being in proximity if the
7 shortest distance between signals was ≤ 80 nm.
8
9 **Intracellular killing assay.**
10 Assessment of intracellular pneumococcal viability was carried out as previously
11 described (10). After the indicated time points macrophages were incubated in RPMI
12 containing 20µg ml^{-1}gentamicin (Sanofi) and 50µU penicillin (Sigma) for 30 min to
13 kill extracellular bacteria before being lysed with 2% saponin for 12 min. Lysates
14 were diluted to 1ml in PBS, and intracellular bacterial numbers determined by Miles-
15 Misra surface viable count. All killing assays were performed in duplicate wells.
16 Early bacterial recovery (≤ 4 h) is a function of both initial phagocytosis and early
17 intracellular killing but correlates well with assessment of phagocytosis by
18 microscopy based analysis and estimation of phagocytic index (1, 2, 18, 19). To
19 assess the kinetics of intracellular bacterial killing a 'pulse-chase' design was
20 performed in which extracellular bacteria were killed with gentamicin/penicillin and
21 then cultures were placed in RPMI containing vancomycin (0.75µg ml^{-1}; Sigma), to
22 ensure extracellular bacteria remained undetectable with an antimicrobial that lacked
23 significant intracellular penetration, before macrophage lysis at the indicated time
24 points as above (Fig. 4E). In experiments to assess killing over a fixed time interval,
25 internalization of bacteria was measured at the first time point, while duplicate wells

were incubated with vancomycin for a further 2 h before macrophage lysis. At all time-points, surface viable counts were also performed on media supernatants to confirm antibiotic killing of extracellular bacteria (Fig. 4H). In experiments to assess the rate of ongoing bacterial internalization, cultures at the indicated time points were incubated with 20μg ml^{-1}gentamicin and 50μU penicillin for 30 min to kill extracellular bacteria before being split into two sets. The first were incubated with vancomycin and the kinetics of intracellular killing measured and the second set received a second pulse with a streptomycin resistant derivative of D39, FP58, at an MOI of 10, in the presence of 10μg ml^{-1}streptomycin (Fig. 4I). Two hours after the addition of this second pulse, extracellular bacteria were killed with penicillin and gentamicin as above and cells were lysed using saponin as above. Lysates were plated out on blood agar plates with or without streptomycin (10μg ml^{-1}), to ascertain the number of intracellular bacteria originating from the second pulse over the preceding 2 h. Assays for intracellular killing of *S. aureus* were similar except that initial killing of extracellular bacteria used lysostaphin at 20 μg ml^{-1} (instead of gentamicin and penicillin) and used lysostaphin at 2 μg ml^{-1} to maintain undetectable extracellular bacteria in a pulse-chase design to measure the kinetics of intracellular killing or the killing over a fixed time interval (20). Surface viable counts confirmed killing of extracellular bacteria with these approaches. To measure ongoing internalization extracellular bacteria were killed with kanamycin at 50 μg $ml^{-1}$and then cells received a second 'pulse' of bacteria with kanamycin resistant *S. aureus* (KanR) in the presence of media containing 50μg ml^{-1} kanamycin. Two hours after the second 'pulse', 20μg ml^{-1}lysostaphin was added for 30 minutes to kill extracellular KanR bacteria, the cells were lysed and lysates plated out in the presence or absence of 50μg ml^{-1} kanamycin (Fig. 2g).

1

2 **Reconstitution of Apoptosis**

3 Apoptosis was reconstituted *in vitro* with clodronate-encapsulated liposomes (5 mg ml^{-1}

4 clodronate) or 0.2 µM ABT-737, 20µM AT101, 20µM UMI-77 or 20µM Sabutoclax

5 (all Selleck Chemicals). Clodronate was a gift of Roche Diagnostics GmbH,

6 Mannheim, Germany. *In vivo* apoptosis of AM was reconstituted in transgenic mice

7 using a modified clodronate-liposome protocol and clodronate containing liposomes

8 supplied by Dr Nico von Rooijen (UMC Amsterdam) (21). *In vivo* reconstitution of

9 apoptosis was achieved using the Bcl-2 specific agent ABT-263 (50mg kg^{-1}, ip), a

10 derivative of ABT-737, and sabutoclax (5mg kg^{-1}, ip), a pan-Bcl-2 inhibitor with

11 inhibitory activity against Mcl-1 (22-24). Doses of all compounds were selected as

12 doses that overcame intrinsic resistance to apoptosis and induced apoptosis in

13 transgenic cells at comparable levels to bacterial infection in non-transgenic cells in the

14 absence of compound.

15

16 **SDS-Page and western blot**

17 Whole cell extracts were isolated using SDS-lysis buffer as described before (10) and

18 equal protein loaded per lane. Proteins were separated by SDS gel electrophoresis,

19 blotted onto a PVDF membrane, and blocked for 60 min at room temperature in PBS

20 containing 0.05% Tween with 5% (v/w) skim milk powder. Membranes were incubated

21 overnight at 4°C with antibodies against human Mcl-1 (mouse monoclonal; 1:1000; BD

22 Pharmingen) (25), mouse Mcl-1 (rabbit polyclonal; 1:1000; Rockland), human/mouse

23 Mcl-1 (rabbit polyclonal SC-19; 1:1000; Santa Cruz), cytochrome *c* (mouse

24 monoclonal clone 7H82C12 IgG2b; 1:1000; BD Pharmingen), cathepsin B (mouse

25 monoclonal clone CA10 IgG2a; 1:1000; Abcam) or β-actin (rabbit polyclonal; 1:5000;

Sigma). Proteins were detected using HRP-conjugated secondary antibodies (1:2000; Dako) and ECL (Amersham Pharmacia). Bands were quantified using Image J 1.32 software (NIH). Fold change from mock-infected was calculated and normalized to the fold change in actin.

Caspase activation

Cellular caspase activity was measured using the Caspase-Glo 3/7 assay (Promega) according to manufacturer's instructions. Luminescence was measured on a Varioskan Flash multimode reader (Thermo Scientific).

Cathepsin D Activation

Cathepsin D activity was measured using a fluorometric cathepsin D activity assay kit (Abcam) in accordance with the manufacturer's instructions (8). Fluorescence was measured on a Varioskan Flash multimode reader (Thermo Scientific). Cathepsin D activity in each sample was expressed as percentage of a comparative sample that had been treated with 500 µM pepstatin A to act as a negative control.

Apoptosis

Nuclear fragmentation and condensation indicative of apoptosis were detected using 4′6′-diamidino-2-phenylindole (DAPI) (1).

Cytokine ELISA

Cytokines in BMDM supernatants were measured with Ready-SET-Go ELISA reagent sets (eBioscience, San Diego, CA) for mouse tumor necrosis factor (TNF),

1 IL-1β and IL-6 in accordance with the manufacturer's protocols. Limits of detection

2 were 8, 8 and 4 pg/ml respectively.

3

4 **Histopathology of murine tissue**

5 Histopathological analysis of tissue sections from mice for analysis of tissue

6 architecture was performed by a pathologist (SC), blinded to the origin of samples, as

7 previously described using Zeiss Axoplan 2E microscope (Zeiss, Oberkochen,

8 Germany) (2). Spleen and lung were visualised with 10X and 20X objective

9 respectively.

10

11 **References**

12 1. Dockrell DH, Lee M, Lynch DH, Read RC. Immune-mediated phagocytosis and
13 killing of Streptococcus pneumoniae are associated with direct and bystander
14 macrophage apoptosis. *J Infect Dis* 2001; 184: 713-722.
15 2. Dockrell DH, Marriott HM, Prince LR, Ridger VC, Ince PG, Hellewell PG, Whyte
16 MK. Alveolar macrophage apoptosis contributes to pneumococcal clearance in
17 a resolving model of pulmonary infection. *J Immunol* 2003; 171: 5380-5388.
18 3. Iannelli F, Chiavolini D, Ricci S, Oggioni MR, Pozzi G. Pneumococcal surface
19 protein C contributes to sepsis caused by Streptococcus pneumoniae in mice.
20 *Infect Immun* 2004; 72: 3077-3080.
21 4. Marriott HM, Bingle CD, Read RC, Braley KE, Kroemer G, Hellewell PG, Craig
22 RW, Whyte MK, Dockrell DH. Dynamic changes in Mcl-1 expression
23 regulate macrophage viability or commitment to apoptosis during bacterial
24 clearance. *J Clin Invest* 2005; 115: 359-368.
25 5. Shipley JM, Wesselschmidt RL, Kobayashi DK, Ley TJ, Shapiro SD.
26 Metalloelastase is required for macrophage-mediated proteolysis and matrix
27 invasion in mice. *Proc Natl Acad Sci U S A* 1996; 93: 3942-3946.
28 6. Cotter MJ, Norman KE, Hellewell PG, Ridger VC. A novel method for isolation of
29 neutrophils from murine blood using negative immunomagnetic separation.
30 *Am J Pathol* 2001; 159: 473-481.
31 7. Tulone C, Uchiyama Y, Novelli M, Grosvenor N, Saftig P, Chain BM.
32 Haematopoietic development and immunological function in the absence of
33 cathepsin D. *BMC Immunol* 2007; 8: 22.
34 8. Bewley MA, Marriott HM, Tulone C, Francis SE, Mitchell TJ, Read RC, Chain B,
35 Kroemer G, Whyte MK, Dockrell DH. A cardinal role for cathepsin d in co-
36 ordinating the host-mediated apoptosis of macrophages and killing of
37 pneumococci. *PLoS pathogens* 2011; 7: e1001262.
38 9. Ojielo CI, Cooke K, Mancuso P, Standiford TJ, Olkiewicz KM, Clouthier S,
39 Corrion L, Ballinger MN, Toews GB, Paine R, 3rd, Moore BB. Defective

phagocytosis and clearance of Pseudomonas aeruginosa in the lung following bone marrow transplantation. *J Immunol* 2003; 171: 4416-4424.

10. Marriott HM, Ali F, Read RC, Mitchell TJ, Whyte MK, Dockrell DH. Nitric oxide levels regulate macrophage commitment to apoptosis or necrosis during pneumococcal infection. *The FASEB journal : official publication of the Federation of American Societies for Experimental Biology* 2004; 18: 1126-1128.
11. Hiraoka W, Vazquez N, Nieves-Neira W, Chanock SJ, Pommier Y. Role of oxygen radicals generated by NADPH oxidase in apoptosis induced in human leukemia cells. *J Clin Invest* 1998; 102: 1961-1968.
12. Mukhopadhyay P, Rajesh M, Hasko G, Hawkins BJ, Madesh M, Pacher P. Simultaneous detection of apoptosis and mitochondrial superoxide production in live cells by flow cytometry and confocal microscopy. *Nat Protoc* 2007; 2: 2295-2301.
13. Gunsolus IL, Hu D, Mihai C, Lohse SE, Lee CS, Torelli MD, Hamers RJ, Murhpy CJ, Orr G, Haynes CL. Facile method to stain the bacterial cell surface for super-resolution fluorescence microscopy. *Analyst* 2014; 139: 3174-3178.
14. Ostrowski PP, Fairn GD, Grinstein S, Johnson DE. Cresyl violet: a superior fluorescent lysosomal marker. *Traffic* 2016; 17: 1313-1321.
15. Bewley MA, Preston JA, Mohasin M, Marriott HM, Budd RC, Swales J, Collini P, Greaves DR, Craig RW, Brightling CE, Donnelly LE, Barnes PJ, Singh D, Shapiro SD, Whyte MKB, Dockrell DH. Impaired Mitochondrial Microbicidal Responses in Chronic Obstructive Pulmonary Disease Macrophages. *Am J Respir Crit Care Med* 2017; 196: 845-855.
16. Dunn KW, Kamocka MM, McDonald JH. A practical guide to evaluating colocalization in biological microscopy. *Am J Physiol Cell Physiol* 2011; 300: C723-742.
17. McCloy RA, Rogers S, Caldon CE, Lorca T, Castro A, Burgess A. Partial inhibition of Cdk1 in G 2 phase overrides the SAC and decouples mitotic events. *Cell Cycle* 2014; 13: 1400-1412.
18. Gordon SB, Irving GR, Lawson RA, Lee ME, Read RC. Intracellular trafficking and killing of Streptococcus pneumoniae by human alveolar macrophages are influenced by opsonins. *Infect Immun* 2000; 68: 2286-2293.
19. Jubrail J, Morris P, Bewley MA, Stoneham S, Johnston SA, Foster SJ, Peden AA, Read RC, Marriott HM, Dockrell DH. Inability to sustain intraphagolysosomal killing of Staphylococcus aureus predisposes to bacterial persistence in macrophages. *Cellular microbiology* 2016; 18: 80-96.
20. Schuhardt VT, Schindler CA. Lysostaphin Therapy in Mice Infected with Staphylococcus Aureus. *J Bacteriol* 1964; 88: 815-816.
21. Van Rooijen N, Sanders A. Liposome mediated depletion of macrophages: mechanism of action, preparation of liposomes and applications. *J Immunol Methods* 1994; 174: 83-93.
22. Bajwa N, Liao C, Nikolovska-Coleska Z. Inhibitors of the anti-apoptotic Bcl-2 proteins: a patent review. *Expert Opin Ther Pat* 2012; 22: 37-55.
23. Dash R, Azab B, Quinn BA, Shen X, Wang XY, Das SK, Rahmani M, Wei J, Hedvat M, Dent P, Dmitriev IP, Curiel DT, Grant S, Wu B, Stebbins JL, Pellecchia M, Reed JC, Sarkar D, Fisher PB. Apogossypol derivative BI-97C1 (Sabutoclax) targeting Mcl-1 sensitizes prostate cancer cells to mda-7/IL-24-mediated toxicity. *Proc Natl Acad Sci U S A* 2011; 108: 8785-8790.

24. Speir M, Lawlor KE, Glaser SP, Abraham G, Chow S, Vogrin A, Schulze KE, Schuelein R, O'Reilly LA, Mason K, Hartland EL, Lithgow T, Strasser A, Lessene G, Huang DC, Vince JE, Naderer T. Eliminating Legionella by inhibiting BCL-XL to induce macrophage apoptosis. *Nat Microbiol* 2016; 1: 15034.

25. Yang T, Kozopas KM, Craig RW. The intracellular distribution and pattern of expression of Mcl-1 overlap with, but are not identical to, those of Bcl-2. *The Journal of cell biology* 1995; 128: 1173-1184.

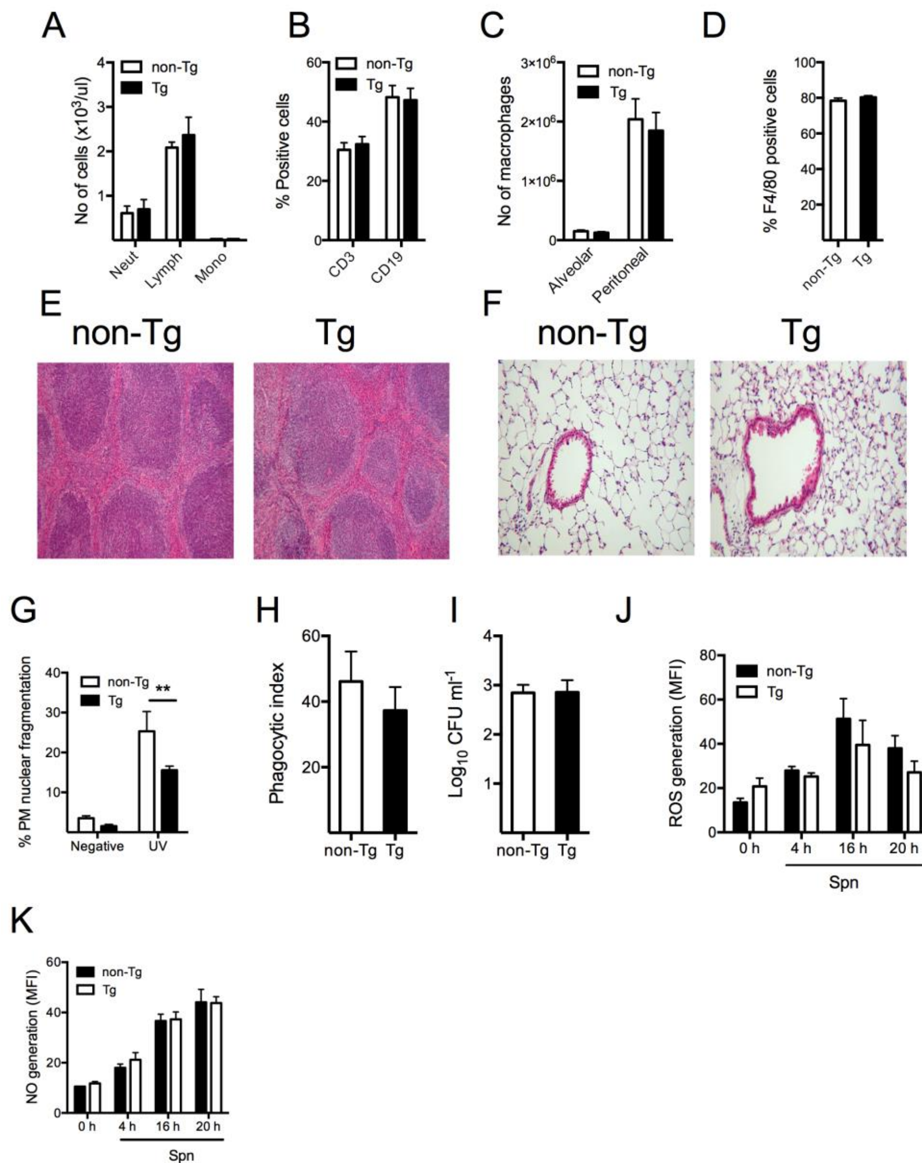

Figure E1: hMcl-1 transgenic mice lack gross immunological or pulmonary phenotypes and have unaltered early immune responses.

(A) Peripheral blood was taken from naïve (unchallenged) CD68.hMcl-1 non-transgenic (non-Tg) or transgenic (Tg) mice, and total cell counts were performed for neutrophils (Neut), lymphocytes (Lymph) and monocytes (Mono), n=4. ***(*B)** Spleen cells from non-Tg or Tg mice were harvested and the percentage of $CD3^+$ T-

lymphocytes (CD3) and $CD19^+$ B-lymphocytes (CD19) assessed by flow cytometry, n=7. **(C)** The total number of macrophages in alveolar and peritoneal lavage of naïve non-Tg and Tg mice, n=9. **(D)** BMDM from non-Tg or Tg mice were differentiated for 14 d and the percentage of macrophages positive for surface expression of the murine macrophage marker F4/80 was assessed by flow cytometry, n=4. **(E-F)** Hematoxylin and eosin stained spleens (E) and lungs (F) from non-Tg or Tg mice were reviewed histopathologically. Tg spleens and lungs displayed normal features. Images are representative of three organs analyzed per group. **(G)** Peritoneal (PM) macrophages from non-Tg or Tg mice were left untreated (negative), or UV treated. 8 h after UV exposure, apoptosis was assessed by nuclear fragmentation, n=6, **= p<0.01, ***= p<0.001 2-way ANOVA. **(H-I)** BMDM from non-Tg or Tg mice were challenged with latex beads (H) or serotype 2 *S. pneumoniae* (Spn) (I). Four hours post-challenge, internalization of beads was analyzed by microscopy, n=9, or viable intracellular colony forming units (CFU) were determined, n=5. **(J-K)** BMDM from non-Tg or Tg mice were challenged with serotype 2 *S. pneumoniae* (Spn). At the designated time post-challenge, production of reactive oxygen species (ROS) (J) and nitric oxide (NO) (K) was measured by flow cytometry and median fluorescence intensity (MFI) recorded. For both experiments, n=3. In all experiments, there were no significant differences between groups.

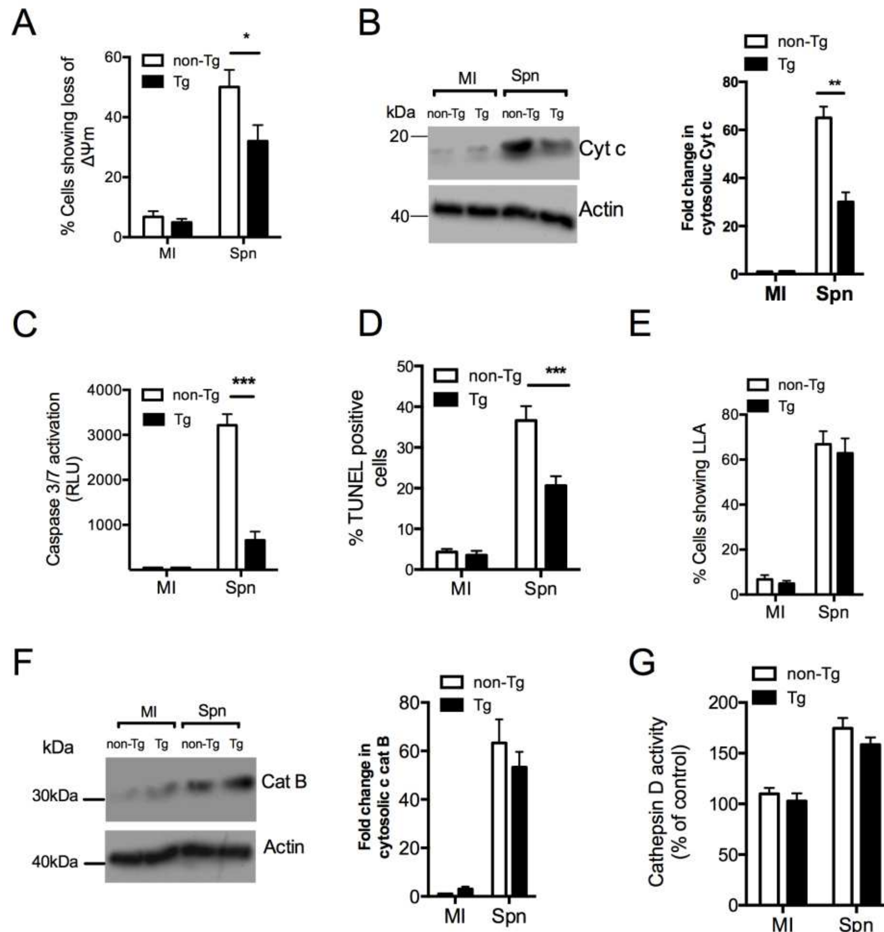

1 **Figure E2: Mcl-1 modifies the mitochondrial pathway of apoptosis but not**
2 **upstream phagolysosomal events in macrophages following bacterial challenge.**
3 Bone marrow-derived macrophages (BMDM) from CD68.hMcl-1 non-transgenic
4 (non-Tg) or CD68.hMcl-1 transgenic (Tg) mice were mock-infected (MI) or
5 challenged with serotype 2 *S. pneumoniae* (Spn). **(A-D)** 16 h post-challenge cells
6 were assessed to determine either (A) the percentage of cells with loss of
7 mitochondrial inner transmembrane potential ($\Delta\psi_m$) by flow cytometry, n=4, (B) were
8 fractionated into membrane and cytosolic fractions and the cytosolic fraction probed
9 for cytochrome c, as a marker of mitochondrial outer membrane permeabilization, (C)
10 were assessed for caspase 3/7 activation measuring relative luminescence units
11 (RLU), n=9, or (D) were assessed for DNA cleavage at 20 h by TUNEL staining,
12 n=4. **(E-F)** 16 h post-challenge cells were assessed to determine (E) the percentage of
13 cells with loss of lysosomal acidification (LLA) by flow cytometry, n=4 or (F)
14 fractionated and cytosolic fractions probed for cathepsin B, as a marker of lysosomal
15 membrane permeabilization, by western blot. **(G)** 8 h post-challenge cells were
16 assessed for cathepsin D activity, n=4. For all experiments, *= p<0.05***=p<0.001,
17 2-way ANOVA. Blots are representative of four independent experiments

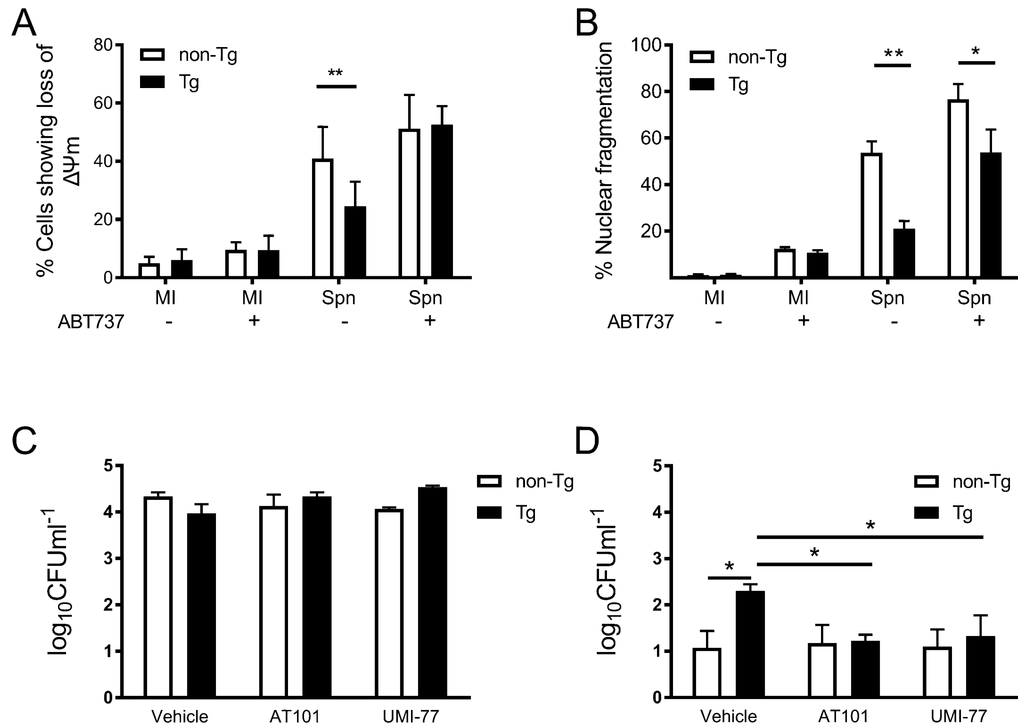

1

2 **Figure E3: BH3 mimetics reconstitute apoptosis-associated killing.**

3 **(A-B)** Bone marrow-derived macrophages (BMDM) from CD68.hMcl-1 non-
4 transgenic (non-Tg) or CD68.hMcl-1 transgenic (Tg) mice were mock-infected (MI) or
5 challenged with serotype 2 *S. pneumoniae* (Spn) in the presence (+) or absence (-) of
6 ABT737. (A) 16 h post-challenge cells were assessed for loss of inner mitochondrial
7 transmembrane potential ($\Delta\psi_m$) by flow cytometry and the percentage of cells with loss
8 of $\Delta\psi_m$ recorded, n=6. (B) At 20 h post-challenge cells were assessed for apoptosis, as
9 assessed by nuclear fragmentation, n=6. **(C-D)** BMDM were infected with serotype 2
10 *S. pneumoniae* after treatment with BH3 mimetics AT101 or UMI-77 or vehicle control
11 and number of viable intracellular bacteria assessed at (C) 4h, n=3 or (D) 20h, n=4. In
12 all experiments *= $p<0.05$, **= $p<0.01$; 2-way ANOVA.

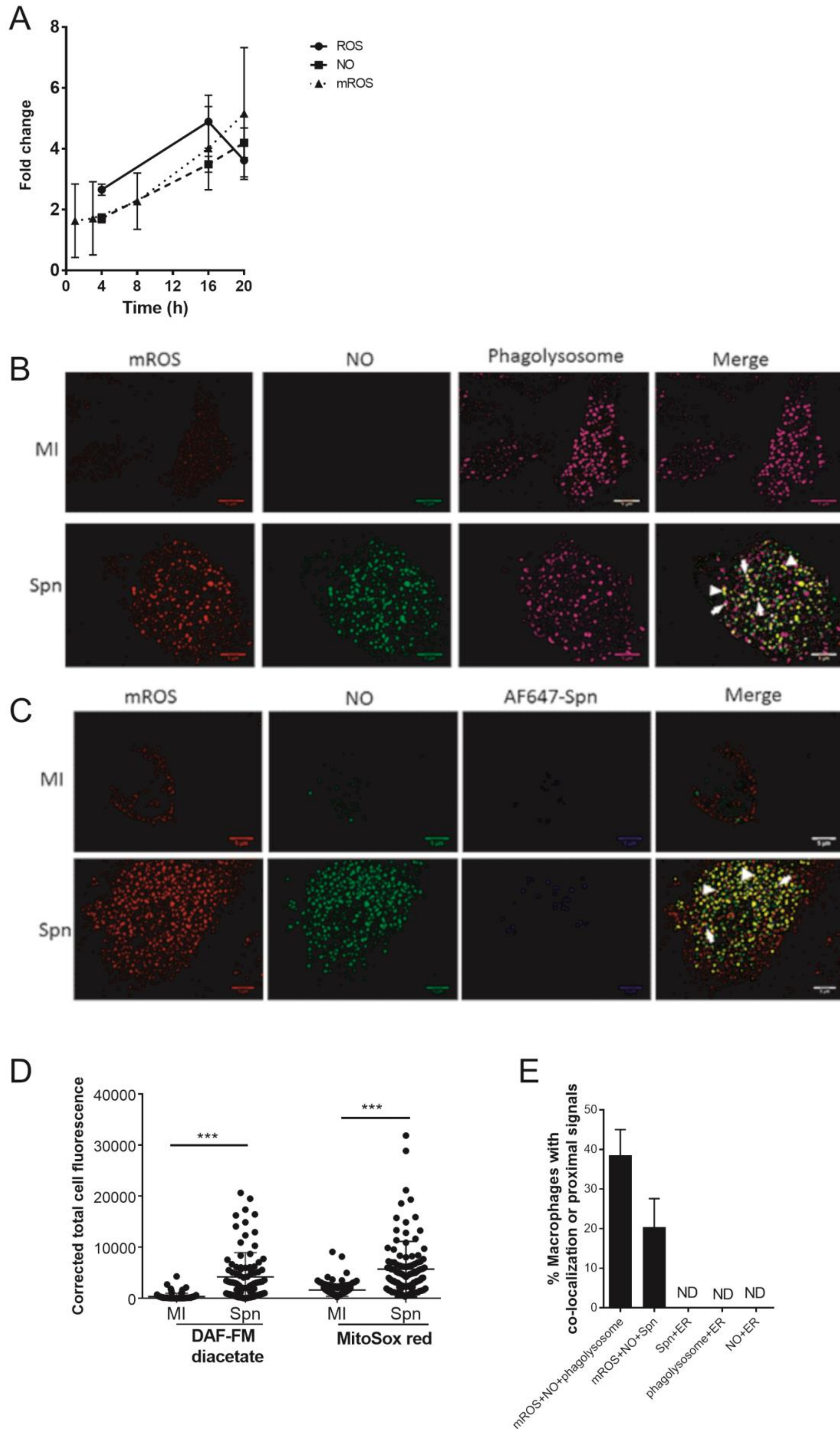

1

1 **Figure E4: Macrophages mitochondrial ROS and NO colocalize with *S.*
2 *pneumoniae* in the phagolysosomal compartment.**
3
4 **(A)** Bone marrow-derived macrophages (BMDM) from CD68.hMcl-1 non-transgenic
5 mice were challenged with serotype 2 *S. pneumoniae* (Spn). At the designated times
6 post challenge production of reactive oxygen species (ROS), nitric oxide (NO) and
7 mitochondrial reactive oxygen species (mROS) were measured by flow cytometry,
8 n=3. **(B-E)** BMDM were exposed to unlabelled or Alexa Fluor-647 conjugated
9 succinimidyl ester labelled opsonized Spn (AF647-Spn) for 16 h. mROS was stained
10 with MitoSOX-red and NO stained with 4-Amino-5-Methylamino-2´, 7´-
11 Difluorofluorescein (DAF-FM) diacetate and phagolysosomes with cresyl violet
12 acetate. Figure (B) shows the representative fluorescence images for mROS (red), NO
13 (green) and phagolysosomes (pink) in mock-infected (MI) BMDM (upper panel) and
14 BMDM challenged with unlabelled Spn (lower panel). The co-localization signals
15 between mROS and NO (yellow pixels) are labelled by the triangular arrows and the
16 co-localization signals with phagolysosomes (white pixels) are labelled by the closed
17 head arrows. Figure (C) shows the representative fluorescence images of mROS (red),
18 NO (green) and AF647- Spn (blue) in MI (upper panel) and AF647-Spn exposed
19 BMDM (lower panel). The co-localization signals between mROS, NO and
20 intracellular AF647- Spn (yellow pixels) are shown by the triangular arrows and
21 proximal signals are labelled by the closed head arrows in the merged image. Scale
22 bars = 5 µm. Figure (D) shows the corrected total cell fluorescence intensity (CTCF)
23 for DAF-FM diacetate and MitoSOX red staining in MI and Spn exposed BMDM
24 from these experiments. Figure (E) shows the percentages of macrophages which
25 show either co-localization signals or proximal signals for the indicated combinations,
26 which also include samples stained to identify endoplasmic reticulum (ER) with ER-
27 Tracker Red. The CTCF and co-localization or proximal signals were measured from
28 three independent experiments. ND = none detected. Data are shows as mean ± SD
29 and statistical analysis was performed with One-way ANOVA and Sidak's multiple
30 comparison post-hoc test. ***p<0.001, n=3.

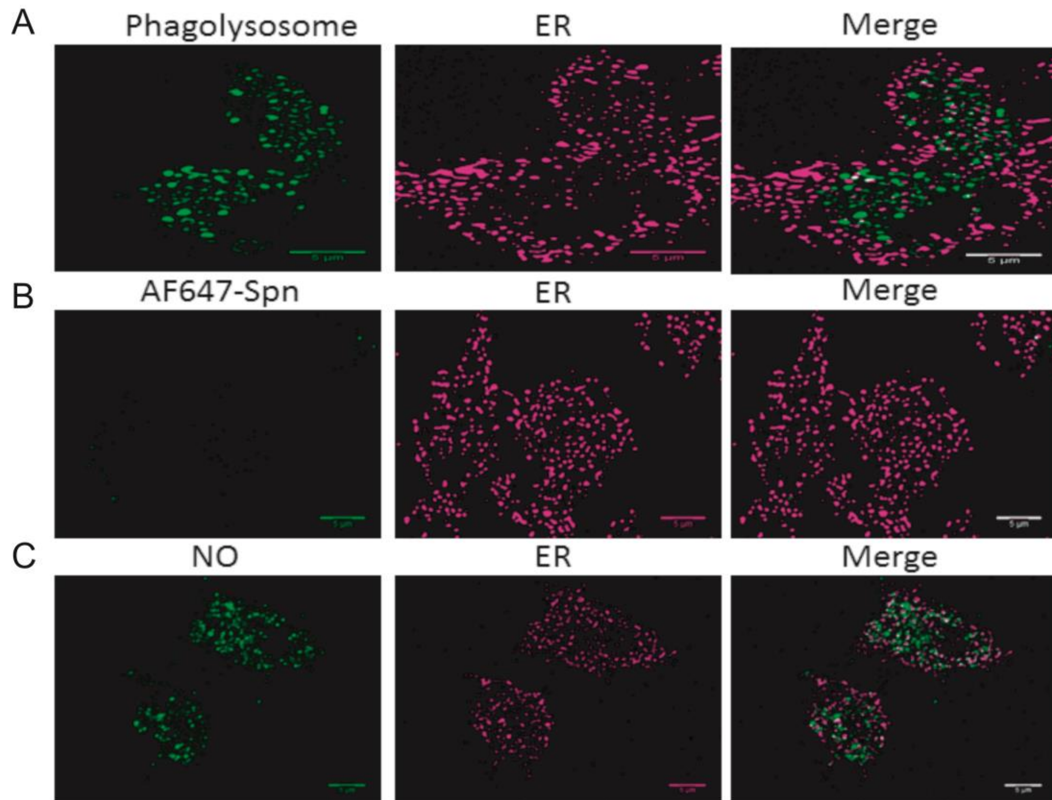

1
2 **Figure E5: Phagolysosomes, Spn and NO do not co-localise with ER.** Mouse bone
3 marrow derived macrophages (BMDM) were challenged with Alexa Fluor-647
4 conjugated succinimidyl ester labelled opsonized *S. pneumoniae* (AF-647 Spn) for 16
5 hours followed by co-staining with ER-Tracker Red and cresyl violet to stain
6 phagolysosomes or 4-Amino-5-Methylamino-2´, 7´-Difluorofluorescein (DAF-FM)
7 diacetate to stain NO. Representative confocal images show no co-localization of ER
8 and phagolysosomes (panel A), ER and AF647-Spn (panel B) or ER and NO (panel C).
9 Scale bars = 5 µm. The images are representative of three independent experiments.

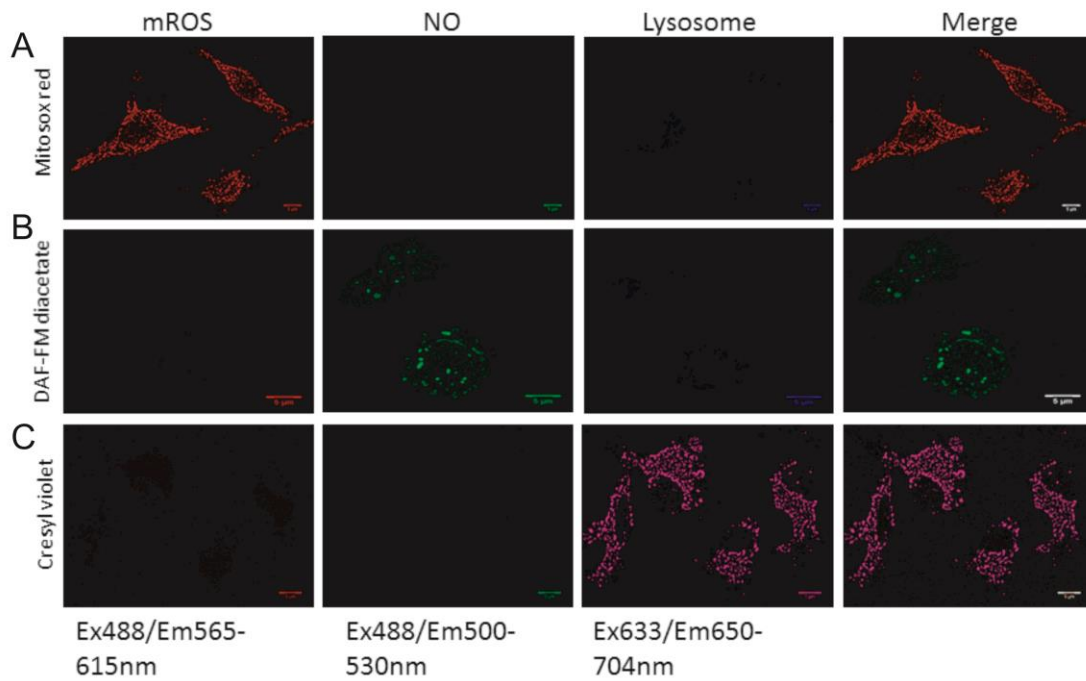

Figure E6: Phagolysosomal staining does not influence detection of nitric oxide or mROS. Mouse bone marrow derived macrophages (BMDM) were challenged with *S. pneumoniae* for 16 hours followed by single staining with either MitoSOX red to detect mROS (A), 4-Amino-5-Methylamino-2´, 7´-Difluorofluorescein (DAF-FM) diacetate to detect NO (B) or with cresyl violet to stain lysosomes/phagolysosomes (C). Images show no significant background in the unstained channels after each stain individually. Scale bars = 5 µm. Images are representative of three independent experiments.

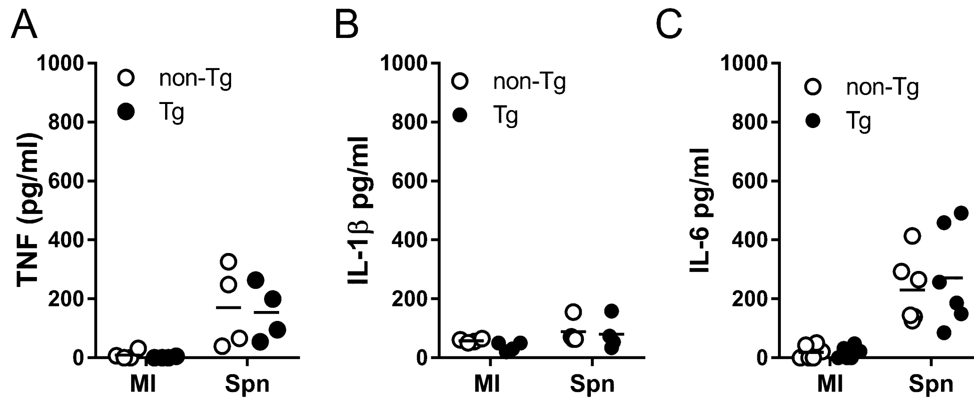

1

2 **Figure E7: Cytokine production is not altered in hMcl-1 transgenic**
3 **macrophages**
4 **(A-C)** Bone marrow-derived macrophages (BMDM) from CD68.hMcl-1 non-
5 transgenic (non-Tg) or CD68.hMcl-1 transgenic (Tg) mice were challenged with
6 serotype 2 *S. pneumoniae* (Spn). 16 h post-challenge production of TNF (A), IL-1β
7 (B), or IL-6 (C) was measured, n=4-6.

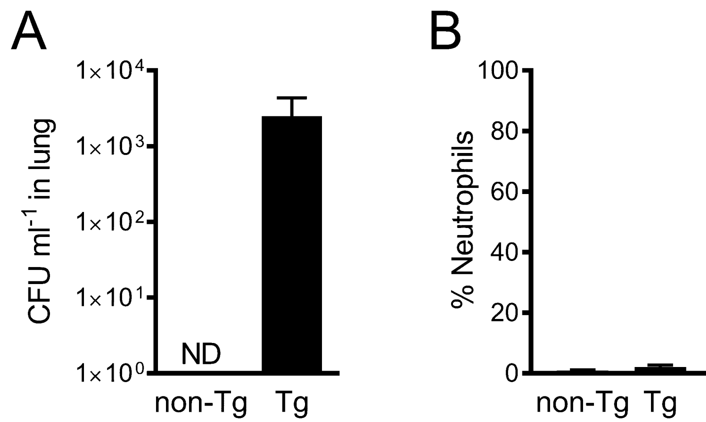

1

2 **Figure E8: Neutrophil depletion**

3 CD68.hMcl-1 transgenic (Tg) mice or CD68.hMcl-1 non-transgenic littermates (non-
4 Tg were treated with Ly6G antibody to deplete circulating neutrophils 24h before
5 intratracheal infection with 10^4 colony forming units of serotype 1 *S. pneumoniae*. 24
6 h post infection the total colony forming units (CFU) in lung (A) were measured and
7 percentage of neutrophils (B) in in bronchoalveolar lavage (BAL) were calculated by
8 analysis of cytospins. ND = none detected, n = 7 per group.

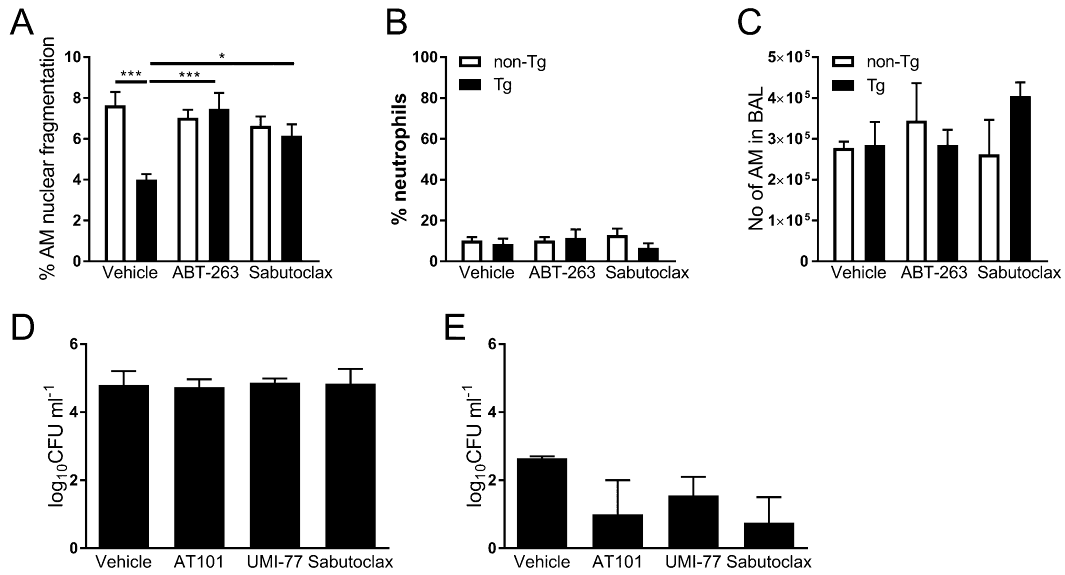

Figure E9: Reconstitution of apoptosis

(A-C) CD68.hMcl-1 transgenic (Tg) mice or CD68.hMcl-1 non-transgenic littermates (non-Tg were instilled intranasally with 10^5 colony forming units of serotype 2 *S. pneumoniae* then immediately treated with ABT-263 or salbutoclax. 24 h post infection the percentage of apoptotic cells (A), percentage of neutrophils (B) and number of alveolar macrophages (AM) in bronchoalveolar lavage (BAL) were calculated by analysis of cytospins , n = 10 per group. (D-E) Human monocyte derived macrophages were challenged with serotype 2 *S. pneumoniae* (Spn) at a multiplicity of infection (MOI) of 10 for 4h (D) or 16 h (E) in the presence of AT101, UMI-77, salbutoclax or vehicle control, n=3, vehicle vs. sabutoclax p=0.05. *** = p<0.001, * = p<0.05 2-way ANOVA with Sidak's multiple comparisons test or One-way ANOVA (D-E only).

1

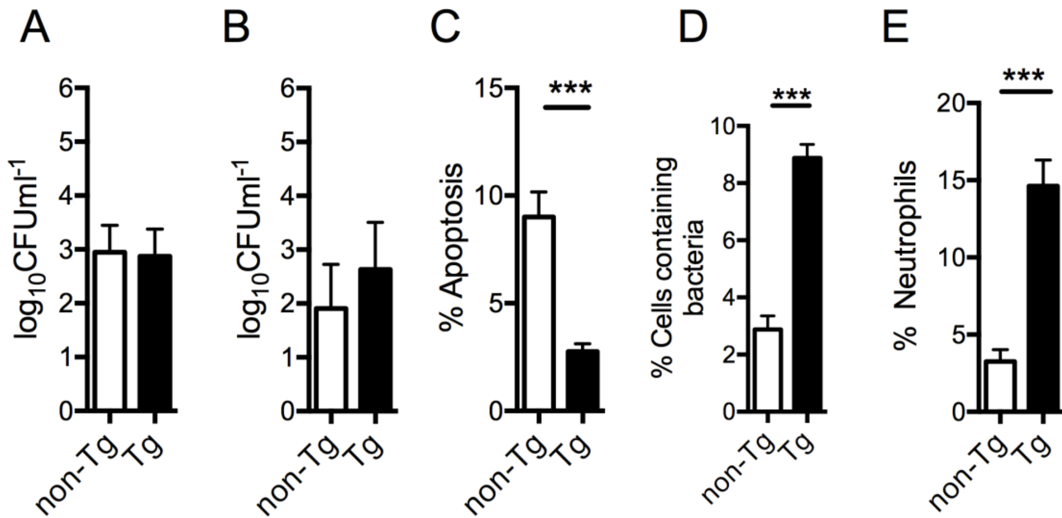

2

3 **Figure E10: Adoptive bone marrow transplant**
4 Mice were transplanted with bone marrow from CD68.hMcl-1 transgenic (Tg) mice or
5 CD68.hMcl-1 non-transgenic littermates (non-Tg). Mice were instilled with 10^4 colony
6 forming units of serotype 1 *S. pneumoniae* for 24 h before the total colony forming
7 units (CFU) in lung (A) and blood (B), percentage of apoptotic cells (C), percentage of
8 cells with associated bacteria (D) and percentage of neutrophils (E) in in
9 bronchoalveolar lavage (BAL) were calculated by analysis of cytospins. n = 8 per
10 group, *** = p<0.05, students t-test.

1

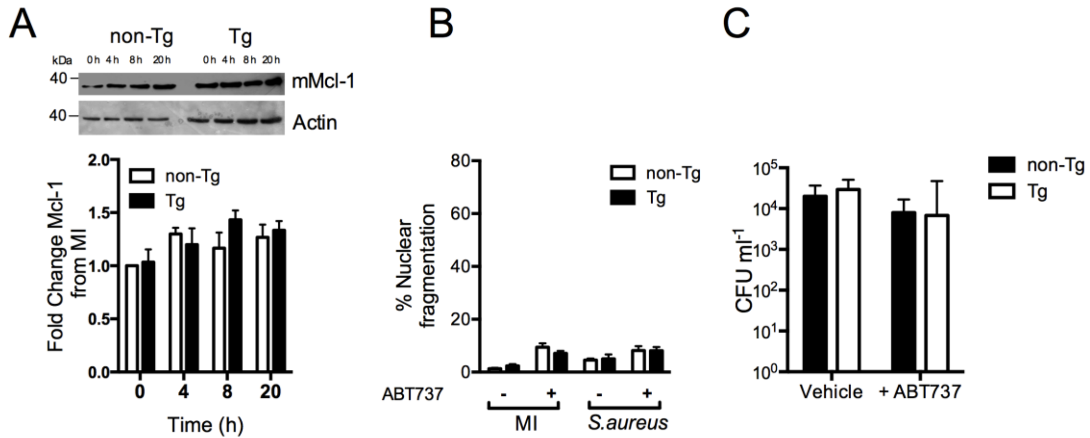

2

3 **Figure E11: *Staphylococcus aureus* infection does not trigger apoptosis-associated**

4 **killing.**

5 **(A)** Bone marrow-derived macrophages (BMDM) form wild-type (non-Tg) or

6 CD68.hMcl-1 transgenic (Tg) were mock-infected (MI) or challenged with *S. aureus*

7 (Sa) at a MOI of 5. Cells were lysed at the designated time and probed for murine (m)

8 Mcl-1. Blot representative of 3 independent experiments and cumulative densitometry

9 presented. **(B-C)** Non-Tg or Tg BMDM were mock-infected (MI) or challenged with

10 *S. aureus* at a multiplicity of infection (MOI) of 5, in the presence (+) or absence (-)

11 of ABT737. 20 h post-challenge cells were assessed for nuclear fragmentation by

12 microscopy (B) and, intracellular colony forming units (CFU) (C). In both

13 experiments, n=3 and no significant differences were noted between groups or over

14 time.